Data Science: Journal of Computing and Applied Informatics
Journal homepage: https://jocai.usu.ac.id

Applied Data Science Framework for Incremental and Interpretable Childhood Growth Risk Screening

Puguh Hiskiawan*[1], Theresia Puspa Wijayanti[2], Srava Chrisdes Antoro[3], Metta Gautama[4]

[1,4]*Data Science, Bunda Mulia University, Jl. Lodan Raya No.2, Jakarta 14430, Indonesia.*
[2]*Informatics, Bunda Mulia University, Jl. Lodan Raya No.2, Jakarta 14430, Indonesia.*
[3]*Artificial Intelligence, Bunda Mulia University, Jl. Lodan Raya No.2, Jakarta 14430, Indonesia.*
*Corresponding Author: phiskiawan@bundamulia.ac.id

ARTICLE INFO

Article history:
Received 11 March 2026
Revised 27 July 2026
Accepted 28 July 2026
Available online 31 July 2026

E-ISSN: 2580-829X
P-ISSN: 2580-6769

How to cite:
Puguh Hiskiawan, Theresia Puspa Wijayanti, Srava Chrisdes Antoro, and Metta Gautama, "Applied Data Science Framework for Incremental and Interpretable Childhood Growth Risk Screening," Data Science : Journal of Computing and Applied Informatics, vol. V10, no. 2, Jul. 2026, doi: 10.32734/jocai.v10i2.24956

ABSTRACT

Childhood growth monitoring is essential for the early identification of children at risk of growth disorders associated with nutritional and health conditions. Conventional screening primarily relies on anthropometric measurements that may not always be consistently obtained in community healthcare settings. This study proposes an applied data science framework for incremental and interpretable childhood growth risk screening by integrating pose-derived body structure features with demographic and anthropometric attributes. Pose landmarks extracted using MediaPipe were combined with age, gender, and body weight to develop predictive models. Six machine learning algorithms were comparatively evaluated using stratified five-fold cross-validation. Logistic Regression achieved the highest predictive performance with a mean ROC-AUC of 0.901. Ablation analysis demonstrated that pose-derived features substantially improved classification performance beyond demographic attributes alone, while odds ratio–based interpretability analysis confirmed the complementary contributions of pose-derived, demographic, and anthropometric features. Although the proposed framework achieved promising performance, the findings should be interpreted in the context of the relatively limited dataset (127 children), and further validation using larger and more diverse pediatric populations is required to improve generalizability.

Keyword: applied data science, growth risk screening, pose estimation, logistic regression, interpretable machine learning.

ABSTRAK

Pemantauan pertumbuhan anak penting untuk mengidentifikasi secara dini anak yang berisiko mengalami gangguan pertumbuhan akibat kondisi gizi dan kesehatan. Metode skrining konvensional umumnya bergantung pada pengukuran antropometri yang tidak selalu dapat dilakukan secara konsisten pada layanan kesehatan berbasis masyarakat. Penelitian ini mengusulkan kerangka kerja applied data science untuk skrining risiko pertumbuhan anak secara incremental dan interpretable dengan mengintegrasikan fitur struktur tubuh berbasis pose estimation dengan atribut demografis dan antropometri. Landmark pose yang diekstraksi menggunakan MediaPipe dikombinasikan dengan variabel usia, jenis kelamin, dan berat badan untuk membangun model prediksi. Enam algoritma machine learning dievaluasi menggunakan stratified five-fold cross-validation. Logistic Regression memberikan performa terbaik dengan nilai rata-rata ROC-AUC sebesar 0.901. Analisis ablation menunjukkan bahwa fitur pose meningkatkan performa klasifikasi dibandingkan atribut demografis saja, sedangkan analisis interpretabilitas berbasis odds ratio mengonfirmasi kontribusi komplementer fitur pose, atribut demografis, dan antropometri. Meskipun menunjukkan performa yang menjanjikan, hasil penelitian ini perlu diinterpretasikan dengan mempertimbangkan keterbatasan dataset yang relatif kecil (127 anak), sehingga diperlukan validasi lebih lanjut pada populasi pediatrik yang lebih besar dan beragam untuk meningkatkan generalisasi model.

Keyword: *applied data science*, skrining risiko pertumbuhan anak, *pose estimation, logistic regression, interpretable machine learning*.

1 Introduction

Childhood growth represents a fundamental indicator of health and developmental well-being during early life. Growth monitoring plays an essential role in identifying children who may experience developmental constraints associated with nutritional deficiency, repeated infections, or unfavourable environmental conditions [1], [2]. The World Health Organization (WHO) provides standardized growth references through the WHO Child Growth Standards, which enable systematic evaluation of children's growth patterns using anthropometric indicators such as length or height relative to age [3]. Children whose height-for-age measurements fall substantially below the reference distribution may experience long-term developmental consequences including reduced cognitive development, limited educational attainment, and increased vulnerability to chronic health conditions later in life. Early identification of children who may face potential growth risk conditions therefore becomes an important component of public health monitoring [4].

Conventional growth assessment programs rely primarily on manual anthropometric measurements performed by trained health workers [5]. Measurement procedures typically involve collecting body height and body weight using standardized equipment in clinical settings or community health services. Practical challenges frequently arise in field environments where measurement equipment may be limited and personnel training may vary across locations. Measurement inaccuracies may occur due to inconsistent procedures, improper posture during measurement, or difficulties in obtaining reliable height measurements for young children. These limitations motivate the exploration of complementary approaches capable of supporting scalable and efficient growth screening systems [6].

Recent developments in computer vision enable automated extraction of structural body information from visual data. Human pose estimation techniques allow detection of anatomical landmarks representing key body joints and body proportions [7]. Frameworks such as MediaPipe provide efficient pose estimation models capable of identifying body landmarks in real time using lightweight architectures. Pose landmarks describing spatial relationships among body parts may capture geometric information related to body proportion and physical development. Integration of pose-derived body structure features with demographic and anthropometric attributes offers a promising direction for developing data-driven childhood growth screening systems [8], [9].

Machine learning approaches have increasingly been adopted to support predictive modeling in healthcare and public health research [10]. Machine learning algorithms such as logistic regression, ensemble tree models, and distance-based methods are capable of learning relationships between multiple predictors and health outcomes [11],[12]. Interpretable models are particularly valuable in health-related applications because they provide transparent explanations regarding how different variables influence prediction outcomes. Model interpretability can support evidence-based decision making and increase trust in automated screening tools deployed in real-world health monitoring systems [13],[14].

Existing studies investigating computer vision and machine learning for childhood growth assessment remain limited in several aspects [15], [16]. Most existing approaches primarily emphasize predictive accuracy while providing limited insight into feature contribution and model interpretability. Furthermore, integration of pose-derived body structure features with conventional demographic and anthropometric attributes has received relatively limited investigation [17]. Comparative evaluation of multiple machine learning algorithms within a unified applied data science framework remains limited, particularly for incremental childhood growth screening applications [18].

This study proposes an Applied Data Science Framework for Incremental and Interpretable Childhood Growth Risk Screening. The framework integrates pose landmark extraction using MediaPipe with demographic and anthropometric attributes including age, gender, and body weight. Six machine learning algorithms are comparatively evaluated for classifying children's growth status into normal growth and growth risk categories based on the WHO 2006 Length/Height-for-Age reference. Model evaluation includes Logistic Regression, Random Forest, Gradient Boosting, XGBoost, K-Nearest Neighbors, and a soft voting ensemble [19], [20]. Additional analyses investigate feature contribution through ablation experiments and model transparency through odds ratio–based interpretability analysis.

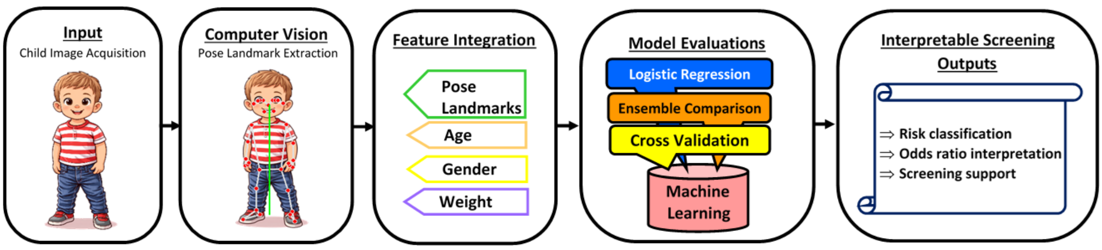

Figure 1. Applied Data Science Framework for Childhood Growth Risk Screening.

Figure 1 presents the overall applied data science framework used in this study. The framework describes the sequential pipeline starting from data acquisition, pose landmark extraction, feature construction, machine learning model training, performance evaluation, and interpretability analysis for childhood growth risk screening.

2 Methods

2.1 Study Design and Dataset

This study adopts an applied data science framework to develop a machine learning–based screening system for childhood growth status classification. The framework integrates computer vision–based pose landmark extraction with demographic and anthropometric attributes to construct predictive models capable of identifying children with potential growth risk conditions [21]. A supervised binary classification setting is applied to categorize children's growth status into normal growth and growth risk [22]. The dataset consists of observations collected from 127 eligible children, where each record includes demographic attributes, anthropometric measurements, and pose-derived visual features. The complete dataset was used for model development and evaluation through stratified five-fold cross-validation, ensuring that each fold preserved the original class distribution while maximizing the use of the available observations.

Table 1. Dataset Characteristics.

Variable	**Description**
Sample size	127 children
Age	age in months
Gender	male / female
Weight	body weight (kg)
Pose landmarks	nose, left shoulder, right shoulder, left hip, right hip
Target label	normal growth / growth risk

Demographic variables include age in months and gender, while anthropometric information is represented by body weight. Pose-related features are extracted from visual images using pose estimation techniques that detect key anatomical landmarks representing upper body structure, including the nose, left shoulder, right shoulder, left hip, and right hip [23]. Growth status labeling follows the WHO 2006 Length/Height-for-Age reference, where children whose height-for-age values fall below −2 standard deviations are categorized as growth risk, while the remaining observations are categorized as normal growth [24]. Table 1 summarizes the demographic variables, anthropometric measurements, pose landmarks, and target labels included in the dataset.

2.2 Pose Landmark Extraction

Human body structure information is extracted using a pose estimation approach that identifies key anatomical landmarks from visual images [25]. Pose estimation enables automated detection of body joints and reference points that describe the spatial configuration of the human body, providing geometric information related to posture and body proportions that may reflect physical growth patterns [26]. This study utilizes the MediaPipe Pose framework, a lightweight and efficient model capable of detecting multiple body landmarks in real time across various body positions and imaging conditions [27]. The framework outputs normalized coordinate representations of anatomical key points, where the horizontal (x) and vertical (y) coordinates are expressed relative to the image dimensions. This normalized representation reduces sensitivity to variations in image resolution and camera distance, providing consistent geometric features for subsequent machine learning analysis.

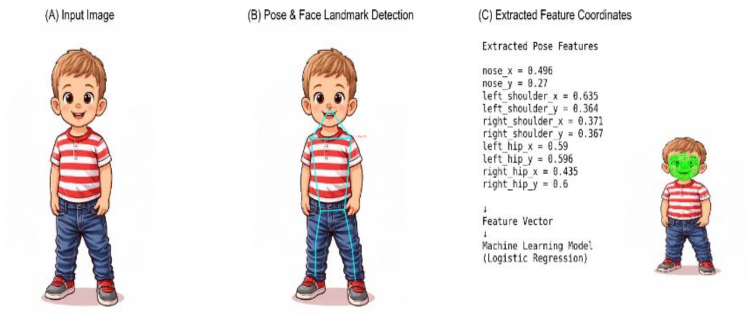

Figure 2. Pose Landmark Extraction Using MediaPipe.

Several upper-body landmarks are selected to represent body proportion characteristics relevant to childhood growth screening, including the nose, left shoulder, right shoulder, left hip, and right hip. These landmarks provide reference points describing vertical alignment and relative body geometry between the upper and lower torso [7], [28]. The extracted landmark coordinates are converted into structured numerical features used as input variables for machine learning models [29]. Figure 2 illustrates the pose landmark extraction process using MediaPipe, where the detected anatomical landmarks are overlaid on the input image to visualize the reference points used for pose-based feature construction.

2.3 Feature Construction

Feature construction integrates pose-derived information with demographic and anthropometric attributes to form a structured feature set for machine learning modelling [30]. Pose landmarks extracted using the MediaPipe framework provide normalized coordinate representations that describe the spatial configuration of key body points, capturing geometric relationships among anatomical landmarks related to body posture and proportions [31]. Pose-based features are derived from selected landmarks including the nose, left shoulder, right shoulder, left hip, and right hip, where each landmark is represented by normalized coordinate values describing its spatial position in the detected pose structure [32].

Demographic attributes are incorporated to represent individual characteristics influencing child growth patterns, where age is represented in months and gender is encoded as a categorical variable. Anthropometric information is represented by body weight, providing additional physiological context related to growth status [33]. These pose-based, demographic, and anthropometric attributes are integrated into a unified feature vector used as input for machine learning models, enabling the models to learn relationships between body geometry, individual characteristics, and childhood growth status classification.

2.4 Machine Learning Models

Machine learning models are employed to learn relationships between pose-derived features, demographic attributes, anthropometric measurements, and children's growth status [34]. Multiple classification algorithms are evaluated to identify a predictive model capable of accurately distinguishing between normal growth and growth risk conditions. Model comparison within the proposed framework allows systematic evaluation of different learning paradigms, including linear models, tree-based ensemble methods, distance-based classifiers, and ensemble voting strategies [35],[36]. Logistic Regression is included as a baseline linear model due to its strong interpretability and suitability for binary classification problems [37]. The probability of the positive class (growth risk) is estimated using the logistic function in Equation (1)

$$P(y=1|x)=\frac{1}{1+e^{-(\beta_0+\beta_1x_1+\beta_2x_2+\cdots+\beta_nx_n)}} \quad (1)$$

where $P(y=1|x)$ represents the predicted probability of the growth risk class, x_i denotes the input feature variables, and β_i represents the corresponding model coefficients learned during training. Tree-based ensemble models are also evaluated due to their ability to capture nonlinear feature relationships [38]. Random Forest aggregates predictions from multiple decision trees built on bootstrapped samples, while Gradient Boosting and XGBoost sequentially construct trees to reduce previous prediction errors and capture complex feature interactions [39]. In addition, K-Nearest Neighbors (KNN) is included as a distance-based classifier that assigns class labels based on similarity among observations in the feature space [40]. A Soft Voting Ensemble combines the predicted probabilities of multiple base classifiers to improve predictive stability through model integration.

2.5 Model Evaluation Metrics

Model performance evaluation assesses the ability of machine learning algorithms to correctly classify children's growth status into normal growth and growth risk categories using stratified five-fold cross-validation. Several standard classification metrics are employed to provide a comprehensive assessment of predictive performance, including accuracy, precision, recall, and F1-score, which measure overall classification correctness, reliability of positive predictions, detection capability for growth risk cases, and the balance between precision and recall [41]. These metrics provide complementary perspectives for evaluating the effectiveness of classification models

Receiver Operating Characteristic (ROC) analysis is also used to assess model discrimination capability across different classification thresholds. The ROC curve illustrates the relationship between the true positive rate and the false positive rate, while the Area Under the ROC Curve (ROC-AUC) summarizes the overall ability of a model to distinguish between normal growth and growth risk conditions [42]. Confusion matrix analysis provides detailed insight into classification outcomes by summarizing true positives, true negatives, false positives, and false negatives, supporting interpretation of model behavior in childhood growth screening scenarios.

2.6 Ablation Study

An ablation study was conducted to examine the contribution of different feature groups used in the proposed framework. The analysis evaluates the contributions of pose-derived features, demographic attributes, and anthropometric measurements to predictive model performance. Systematic inclusion and removal of feature groups enables assessment of their relative contributions to childhood growth status classification [43]. Pose features are derived from anatomical landmarks extracted using the MediaPipe framework, while demographic attributes include age and gender. Anthropometric information is represented by body weight, which provides additional physiological context related to child growth conditions [18].

Several experimental configurations are evaluated, including demographic attributes only, pose-derived features only, pose combined with demographic attributes, and the complete feature set integrating pose, demographic, and anthropometric variables. Comparison across these configurations allows identification of feature groups that contribute most strongly to classification performance [44]. The ablation results provide insight into the contribution of each feature group to the proposed screening framework, while detailed quantitative findings are presented in the Results section.

2.7 Model Interpretability

Model interpretability analysis is conducted to examine how individual features contribute to the classification outcomes produced by the predictive model. Interpretability is particularly important in health-related machine learning applications because transparent models enable researchers and practitioners to understand how input variables contribute to prediction results [45]. Logistic Regression provides an inherently interpretable modelling structure in which each feature coefficient represents the strength and direction of its association with the predicted class. Coefficient interpretation is performed using odds ratio analysis, which transforms logistic regression coefficients into interpretable effect measures that quantify the multiplicative change in the probability of the positive class for a one-unit increase in a given feature while other variables remain constant [46]. Odds ratio values are calculated from the logistic regression coefficients according to Equation (2).

$$OR = e^{\beta} \tag{2}$$

where OR denotes the odds ratio and β represents the coefficient estimated by the logistic regression model. Values greater than one indicate that a feature increases the probability of the growth risk class, while values lower than one indicate a decreasing effect. This interpretation provides intuitive insight into how demographic attributes, anthropometric measurements, and pose-derived features contribute to childhood growth status classification [47]. Visualization of the estimated odds ratios facilitates interpretation of feature contributions, while detailed results of the interpretability analysis are presented in the Results section.

3 Results and Discussion

3.1 Model Performance Comparison

Model performance comparison evaluates the predictive capability of six machine learning algorithms for classifying children's growth status into normal growth and growth risk categories. Model performance was assessed using stratified five-fold cross-validation, and predictive capability was summarized using the mean and standard deviation of the ROC-AUC metric. Table 2 summarizes the comparative performance of the evaluated models. Logistic Regression achieved the highest mean ROC-AUC of 0.901 (±0.066), followed by the Soft Voting Ensemble (0.851), XGBoost (0.830), and Gradient Boosting (0.795). Random Forest (0.700) and K-Nearest Neighbors (0.679) produced comparatively lower predictive performance.

Table 2. Model Performance Comparison Based on ROC-AUC.

Model	Mean ROC-AUC	Std. Dev.
Logistic Regression	**0.901**	0.066
Soft Voting Ensemble	0.851	0.087
XGBoost	0.830	0.107
Gradient Boosting	0.795	0.113
Random Forest	0.700	0.125
K-Nearest Neighbors	0.679	0.101

Performance differences among the evaluated models indicate that the constructed feature representation provides sufficient discriminative information for childhood growth status classification. Logistic Regression outperformed more complex ensemble models, suggesting that the relationships among pose-derived body structure features, demographic attributes, and anthropometric measurements can be effectively represented using a linear decision boundary. These findings support the use of interpretable models for health-related screening applications, where transparency and model explainability are important considerations.

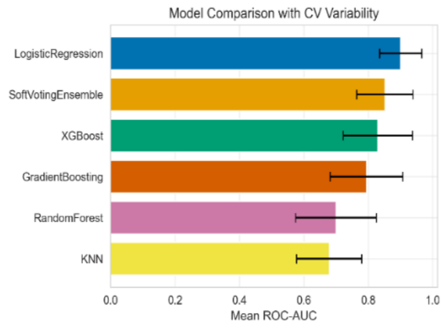

Figure 3. Model comparison based on mean ROC-AUC.

3.2 Feature Contribution Analysis

Feature contribution analysis examines the relative contribution of different feature groups to the proposed classification framework. The ablation study evaluates how demographic attributes, pose-derived landmarks, and anthropometric measurements influence predictive performance through progressive feature integration. Table 3 summarizes the ablation results based on the mean ROC-AUC obtained from stratified five-fold cross-validation. The configuration using only demographic attributes (age and gender) achieved the lowest ROC-AUC of 0.620, indicating that demographic information alone provides limited discriminative capability. Incorporating pose-derived landmarks increased the ROC-AUC to 0.830, demonstrating that body structure information extracted through pose estimation contributes meaningful signals for childhood growth status classification.

Table 3. Ablation Study Results Based on Feature Configurations.

Feature Configuration	Mean ROC-AUC	Std. Dev.
Age + Gender	0.620	0.090
Age + Gender + Pose Landmarks	0.830	0.080
Age + Gender + Pose Landmarks + Weight	**0.901**	0.066

Further improvement was observed when body weight was integrated with demographic attributes and pose landmarks. The complete feature configuration achieved the highest ROC-AUC of 0.901, demonstrating that combining pose-derived body structure, demographic characteristics, and anthropometric measurements provides a more informative representation for childhood growth status classification. Figure 4 illustrates the incremental improvement in ROC-AUC across the evaluated feature configurations, highlighting the complementary contribution of pose landmarks and body weight to predictive performance.

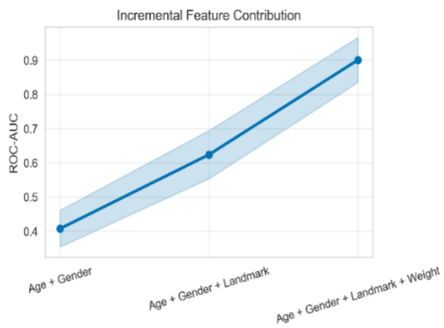

Figure 4. Incremental improvement of ROC-AUC across feature configurations.

3.3 ROC Performance Analysis

Receiver Operating Characteristic (ROC) analysis evaluates the discriminative capability of the evaluated machine learning models in distinguishing between normal growth and growth risk conditions. ROC curves illustrate the trade-off between the true positive rate and the false positive rate across different classification thresholds. Figure 5 compares the ROC curves of the evaluated models, showing that Logistic Regression consistently achieved the highest area under the curve among the tested algorithms. Soft Voting, XGBoost, and Gradient Boosting demonstrated competitive performance, although their ROC curves remained slightly below that of Logistic Regression across most classification thresholds. Random Forest and K-Nearest Neighbors showed comparatively weaker discrimination capability, consistent with the quantitative results reported in Table 2.

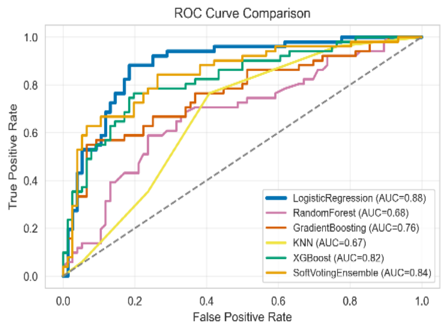

Figure 5. ROC curve comparison of machine learning models.

ROC curve visualization further demonstrates the robustness of Logistic Regression in separating the two growth status categories. The curve of Logistic Regression remains consistently above the other models across the majority of the false positive rate range, indicating stronger classification performance. Figure 6 presents the ROC curves with cross-validation confidence intervals, where the shaded regions represent performance variability across the evaluation folds. Logistic Regression exhibited relatively narrow confidence intervals compared with the other evaluated models, indicating more stable predictive performance across the cross-validation folds.

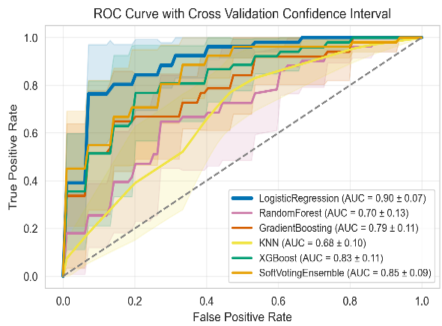

Figure 6. ROC curves with cross-validation confidence intervals.

3.4 Confusion Matrix Analysis

Confusion matrix analysis provides a detailed evaluation of the classification outcomes generated by the best-performing model. Logistic Regression achieved the highest ROC-AUC among the evaluated models and was therefore selected for further analysis of its classification behavior. The confusion matrix summarizes prediction outcomes by reporting true positives, true negatives, false positives, and false negatives. Figure 7 presents the confusion matrix obtained from the Logistic Regression model.

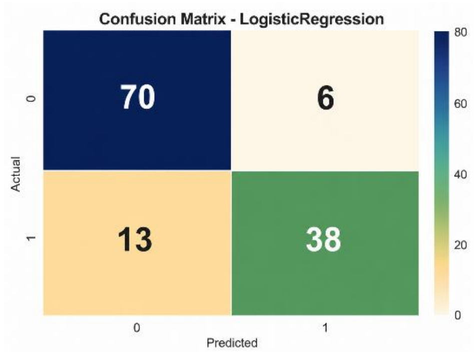

Figure 7. Confusion matrix of the Logistic Regression model.

Results show that most observations were correctly classified, indicating that the proposed model effectively distinguished between children with normal growth and those at growth risk. Although the number of misclassified cases was relatively small, both false positive and false negative predictions were observed. False positive predictions may lead to additional clinical assessment for children who are ultimately identified as having normal growth, whereas false negative predictions represent missed growth risk cases and therefore require particular attention in health screening applications. In the present study, the relatively small number of false negative predictions suggests that the proposed framework maintains a favourable balance between sensitivity and overall predictive performance. Some misclassifications may be attributed to natural variations in body posture, image acquisition conditions, or overlapping physical characteristics between growth categories. These findings demonstrate the potential of the proposed framework as a decision-support tool for early growth risk screening, while confirming that clinical assessment remains essential for final diagnosis. The findings should be interpreted in the context of the relatively limited dataset used in this study. Additional validation using larger and more diverse pediatric populations is required to further assess the generalizability and clinical applicability of the proposed framework. Future implementation of the proposed framework in community healthcare settings would benefit from standardized image acquisition procedures. Health workers should capture frontal full-body images using a consistent camera distance and approximately perpendicular camera angle under adequate lighting conditions to improve the consistency of pose landmark extraction. Establishing standardized image capture protocols may reduce variability caused by field conditions and strengthen the robustness, reproducibility, and practical applicability of the proposed screening framework

3.5 Model Interpretability

Model interpretability analysis provides insight into how individual features contribute to the classification outcomes generated by the Logistic Regression model. Odds ratio analysis was used to quantify the contribution of each feature to the probability of the growth risk class. Values greater than one indicate an increased likelihood of growth risk, whereas values lower than one indicate a reduced likelihood.

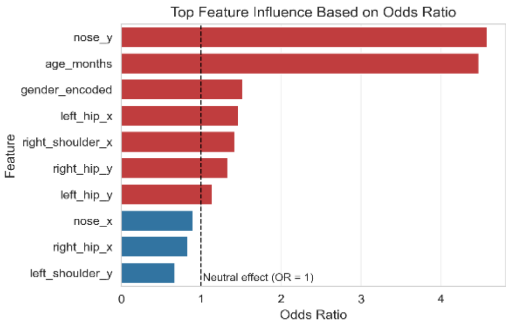

Figure 8. Feature influence based on odds ratio from the Logistic Regression model.

Figure 8 illustrates the most influential features identified by the Logistic Regression model based on their estimated odds ratios. Several pose-derived landmarks appeared among the strongest predictors, indicating that body structure characteristics extracted through pose estimation contributed meaningful complementary information for childhood growth status classification. Age in months also demonstrated substantial influence, reflecting the expected relationship between child age and physical growth patterns. These findings demonstrate that integrating pose-derived, demographic, and anthropometric information enables the proposed framework to capture meaningful patterns associated with childhood growth status. The transparent nature of Logistic Regression further supports its application as a decision-support tool for early growth risk screening.

4 Conclusion

This study presented an interpretable applied data science framework for childhood growth risk screening by integrating pose-derived body structure features with demographic and anthropometric attributes. Pose landmarks extracted through MediaPipe were combined with machine learning algorithms to classify children's growth status. Experimental evaluation of six machine learning algorithms demonstrated that Logistic Regression achieved the highest predictive performance with a mean ROC-AUC of 0.901. Ablation analysis further showed that pose-derived landmarks substantially improved classification performance beyond demographic attributes alone, while odds ratio analysis confirmed the complementary contributions of pose-derived, demographic, and anthropometric features to model predictions. The findings demonstrate that interpretable machine learning can effectively support early childhood growth risk screening by providing transparent predictions while preserving clinical interpretability.

Several limitations should be acknowledged. The dataset remained relatively limited and was collected from a single observational setting, which may restrict the generalizability of the proposed framework. In addition, pose landmark extraction may be affected by variations in body posture, camera positioning, and image acquisition conditions. Future research should validate the proposed framework using larger and more diverse pediatric populations, establish standardized image acquisition protocols for community healthcare implementation, investigate additional pose-based geometric descriptors, and explore advanced representation learning techniques. Integration with mobile or edge-based screening platforms may further enhance the practical applicability of automated childhood growth risk screening in community healthcare settings.

5 Acknowledgements

The authors would like to express their sincere gratitude to Universitas Bunda Mulia for supporting this research. Financial support provided by the Directorate of Research and Community Service (Direktorat Penelitian dan Pengabdian kepada Masyarakat) is gratefully acknowledged.

References

[1] P. Hiskiawan, Y. M. Geasela, H. Heryanto, E. Stephanie, M. Ardianti, and F. A. Sukarno, "Trustworthy Data Science Framework for Non-Invasive Nutritional Screening Using Computer Vision," in *2025 International Conference on Informatics, Multimedia, Cyber and Information System (ICIMCIS)*, 2025, pp. 1743–1748.

[2] P. R. D. Raju M Sairise, "Nutritional Analysis Using Deep Learning: A Revolution in Understanding Dietary Patterns," *Int. J. food Nutr. Sci.*, vol. 11, no. 6, pp. 1176–1186, 2022.

[3] M. H. M. Nawawi, M. S. Ishak, R. F. A. Raes, I. A. Razak, S. Hasan, and A. I. A. Rahim, "The intersection of quality improvement, artificial intelligence and patient safety in healthcare—current applications, challenges and risks, and future directions: a scoping review," Dec. 30, 2025, *AME Publishing Company*. doi: 10.21037/jmai-24-328.

[4] Y. Y. Liu, "Deep learning for microbiome-informed precision nutrition," *Natl. Sci. Rev.*, vol. 12, no. 6, pp. 10–13, 2025, doi: 10.1093/nsr/nwaf148.

[5] A. Budhewar, S. Purbuj, D. Rathod, M. Tukan, and P. Kulshrestha, "Human Behaviour Analysis Using CNN," *SHS Web Conf.*, vol. 194, p. 01001, 2024, doi: 10.1051/shsconf/202419401001.

[6] F. TARLAK and Ö. YÜCEL, "Identification of foods in the breakfast and determination of nutritional facts using deep convolution neural networks," *Food Sci. Technol.*, vol. 43, 2023, doi: 10.5327/fst.10323.

[7] F. E. Sadeq and Z. T. M. Al-Ta'i, "Comparison Between Face and Gait Human Recognition Using Enhanced Convolutional Neural Network," *J. Appl. Eng. Technol. Sci.*, vol. 5, no. 1, pp. 18–30, 2023, doi: 10.37385/jaets.v5i1.2806.

[8] S. Prongnuch, "Face and Hand Gesture Recognition System Using MediaPipe," *J. Eng. Ind. Technol.*, vol. 3, no. August, pp. 46–58, 2025.

[9] Elbert, E. Setyaningsih, and L. Widodo, "Comparative Analysis of Haar Cascade Classifier, Dlib, and Mediapipe for Face Recognition," *ELECTRON J. Ilm. Tek. Elektro*, vol. 6, no. 1, pp. 1–8, 2025, doi: 10.33019/electron.v6i1.240.

[10] R. Tachicart, H. Rezki, A. Korchi, and A. Abatal, "A comparative study of machine learning algorithms for breast cancer diagnosis," Dec. 30, 2025, *AME Publishing Company*. doi: 10.21037/jmai-24-368.

[11] E. Mihajloska *et al.*, "Machine learning approaches for DAS28 score prediction after rituximab treatment in rheumatoid arthritis patients," *J. Med. Artif. Intell.*, vol. 8, Dec. 2025, doi: 10.21037/jmai-24-288.

[12] P. Hiskiawan, C. Chih, C. Zheng, and K. Ye, "Processing of electrical resistivity tomography data using convolutional neural network in ERT - NET architectures," *Arab. J. Geosci.*, pp. 1–14, 2023, doi: 10.1007/s12517-023-11690-w.

[13] Y. M. Geasela, P. Hiskiawan, S. Everlin, and E. A. Chandra, "KECERDASAN BUATAN UNTUK EFISIENSI DAN AKURASI LAYANAN POSYANDU BERBASIS PEMBERDAYAAN MASYARAKAT," *J. Pengabdi. dan Kewirausahaan*, vol. 9, no. 2, pp. 63–72, 2025.

[14] F. S. Akzatria, "Implementation of Artificial Intelligence in Healthcare," *J. Adv. Technol. Multidiscip.*, vol. 02, no. 02, 2023.

[15] S. Tayebi Arasteh *et al.*, "Differential privacy enables fair and accurate AI-based analysis of speech disorders while protecting patient data," *npj Artif. Intell.*, vol. 1, no. 1, p. 37, Nov. 2025, doi: 10.1038/s44387-025-00040-8.

[16] F. J. Kaunang *et al.*, "Sound Engine Based In-situ Environment Leveraging Neural Network Classification Algorithm," in *The 2025 IEEE International Conference on Artificial Intelligence for Learning and Optimization (ICoAILO) Sound*, 2025, pp. 352–358.

[17] B. Kalivaraprasad, M. V.D. Prasad, and N. K. Gattim, "Deep Learning-based Food Calorie Estimation Method in Dietary Assessment: An Advanced Approach using Convolutional Neural Networks," *Int. J. Adv. Comput. Sci. Appl.*, vol. 15, no. 3, pp. 1044–1050, 2024, doi: 10.14569/IJACSA.2024.01503104.

[18] D. Chicco, M. J. Warrens, and G. Jurman, "The coefficient of determination R-squared is more informative than SMAPE, MAE, MAPE, MSE and RMSE in regression analysis evaluation," *PeerJ Comput. Sci.*, vol. 7, pp. 1–24, 2021, doi: 10.7717/PEERJ-CS.623.

[19] R. Tachicart, H. Rezki, A. Korchi, and A. Abatal, "A comparative study of machine learning algorithms for breast cancer diagnosis," *J. Med. Artif. Intell.*, no. Ml, 2025, doi: 10.21037/jmai-24-368.

[20] J. Bajwa, U. Munir, A. Nori, and B. Williams, "Artificial intelligence in healthcare: transforming the practice of medicine," *Artif. Intell. Healthc.*, vol. 8, no. 2, pp. 188–194, 2021, doi: 10.7861/fhj.2021-0095.

[21] K. V. Bharath Kumar, B Purushotham, B. Sushanth Sai, P. Sathish, and M. Shoaib, "Hand and Face Landmarks Detection Using Media Pipe and Ai," *Ijariie.Com*, vol. 11, no. 3, pp. 205–211, 2025.

[22] M. Chakole, S. Sontakke, L. Umredkar, V. Rathod, R. Umate, and S. Dorle, "Real-Time Full-Body Detection Using Computer Vision: Leveraging OpenCV and MediaPipe," *SSRG Int. J. Electr. Electron. Eng.*, vol. 11, no. 11, pp. 231–240, 2024, doi: 10.14445/23488379/IJEEE-V11I11P123.

[23] M. Nazarkevych, V. Lutsyshyn, H. Nazarkevych, L. Parkhuts, and M. Kostiak, "Methods of Face Recognition in Video Sequences and Performance Studies," *CEUR Workshop Proc.*, vol. 3421, pp. 246–253, 2023.

[24] R. U. Karim, S. Mahdi, A. Samin, A. N. Zereen, M. Abdullah-Al-Wadud, and J. Uddin, "Optimizing Stroke Recognition With MediaPipe and Machine Learning: An Explainable AI Approach for Facial Landmark Analysis," *IEEE Access*, vol. 13, no. March, pp. 32636–32660, 2025, doi: 10.1109/ACCESS.2025.3550577.

[25] S. Serengil and A. Özpınar, "A Benchmark of Facial Recognition Pipelines and Co-Usability Performances of Modules," *Bilişim Teknol. Derg.*, vol. 17, no. 2, pp. 95–107, 2024, doi: 10.17671/gazibtd.1399077.

[26] G. Sujatha *et al.*, "Multi-Cnn Model To Evaluate the Performance of Face Detection and Recognition With Facial Feature Detection and Recognition," *J. Theor. Appl. Inf. Technol.*, vol. 103, no. 9, pp. 3548–3560, 2025.

[27] E. Barcic, P. Grd, and I. Tomicic, "Convolutional Neural Networks for Face Recognition: A Systematic Literature Review," *Res. Sq.*, pp. 1–85, 2023, [Online]. Available: https://www.researchsquare.com/article/rs-3145839/v1

[28] I. Frajtag, M. Švaco, and F. Šuligoj, "Evaluation of Facial Landmark Localization Performance in a Surgical Setting," *Mech. Mach. Sci.*, vol. 190, pp. 278–287, 2025, doi: 10.1007/978-3-032-02106-9_31.

[29] F. Bougourzi, F. Dornaika, N. Barrena, C. Distante, and A. Taleb-Ahmed, "CNN based facial aesthetics analysis through dynamic robust losses and ensemble regression," *Appl. Intell.*, vol. 53, no. 9, pp. 10825–10842, 2023, doi: 10.1007/s10489-022-03943-0.

[30] A. K. M. Baareh, "Facial Recognition and Discovery Using Convolution Deep Learning Neural Network," *J. Comput. Sci.*, vol. 20, no. 11, pp. 1559–1568, 2024, doi: 10.3844/jcssp.2024.1559.1568.

[31] Q. Sun and A. Redei, "Knock Knock, Who's There: Facial Recognition using CNN-based Classifiers," *Int. J. Adv. Comput. Sci. Appl.*, vol. 13, no. 1, pp. 9–16, 2022, doi: 10.14569/IJACSA.2022.0130102.

[32] Y. Fan, "The Gesture Recognition Improvement of Mediapipe Model Based on Historical Trajectory Assist Tracking Kalman Filtering and Smooth Filtering," *ACM Int. Conf. Proceeding Ser.*, pp. 641–647, 2024, doi: 10.1145/3703187.3703295.

[33] N. Singh, R. Kumar, B. T. Student, and G. Noida, "FACE & EYE MOTION DETECTION," *Int. J. Nov. Res. Dev.*, vol. 10, no. 4, pp. 8–11, 2025.

[34] S. Zeb, N. FNU, N. Abbasi, and M. Fahad, "AI in Healthcare: Revolutionizing Diagnosis and Therapy," *Int. J. Multidiscip. Sci. Arts*, vol. 3, no. 3, pp. 118–128, Aug. 2024, doi: 10.47709/ijmdsa.v3i3.4546.

[35] A. Maigari, C. Xinying, and Z. Zainol, "Multimodal deep learning breast cancer prognosis models: narrative review on multimodal architectures and concatenation approaches," Dec. 30, 2025, *AME Publishing Company*. doi: 10.21037/jmai-24-146.

[36] F. Mahardhika, M. L. Haryanti, and P. Hiskiawan, "Performance Evaluation of Speech Emotion Recognition Using Hybrid Feature Selection and Machine Learning," in *2025 4th International Conference on Creative Communication and Innovative Technology (ICCIT)*, 2025, pp. 1–7. doi: 10.1109/ICCIT65724.2025.11166879.

[37] M. Nguyen *et al.*, "A predictive tool to forecast the Model for End-Stage Liver Disease score : the ' MELDPredict ' tool," *J. Med. Artif. Intell.*, pp. 0–2, 2025, doi: 10.21037/jmai-24-277.

[38] P. Hiskiawan, J. William, and L. F. Tio Jansel, "A Hybrid Data Science Framework for Forecasting Bitcoin Prices using Traditional and AI Models," *J. Appl. Informatics Comput.*, vol. 9, no. 5, pp. 2089–2101, 2025, doi: https://doi.org/10.30871/jaic.v9i5.10631.

[39] M. Nguyen *et al.*, "A predictive tool to forecast the Model for End-Stage Liver Disease score: the 'MELDPredict' tool," *J. Med. Artif. Intell.*, vol. 8, Dec. 2025, doi: 10.21037/jmai-24-277.

[40] A. Maigari, C. Xinying, and Z. Zainol, "Multimodal deep learning breast cancer prognosis models : narrative review on multimodal architectures and concatenation approaches," *J. Med. Artif. Intell.*, 2025, doi: 10.21037/jmai-24-146.

[41] R. M. Sharma, "Artificial intelligence in medical image analysis and molecular diagnostics: recent advances and applications," Dec. 30, 2025, *AME Publishing Company*. doi: 10.21037/jmai-24-412.

[42] M. R. Shadi, H. Mirshekali, and H. R. Shaker, "Explainable artificial intelligence for energy systems maintenance : A review on concepts , current techniques , challenges , and prospects," *Renew. Sustain. Energy Rev.*, vol. 216, no. March, 2025.

[43] S. Ali *et al.*, "An Efficient Intersection over Union Algorithm for 3D Object Detection," *IEEE Access*, vol. PP, p. 1, 2024, doi: 10.1109/ACCESS.2024.3495761.

[44] M. Lot *et al.*, "Differential privacy enables fair and accurate AI-based analysis of speech disorders while protecting patient data," *npj | Artif. Intell.*, vol. 1, no. 37, pp. 1–16, 2025.

[45] Y. Itaya, J. Tamura, K. Hayashi, and K. Yamamoto, "Asymptotic Properties of Matthews Correlation Coefficient," *Stat. Med.*, vol. 44, no. 1–2, Jan. 2025, doi: 10.1002/sim.10303.

[46] P. Stoica and P. Babu, "Pearson-Matthews correlation coefficients for binary and multinary classification and hypothesis testing," in *Proceedings - IEEE International Conference on Robotics and Automation*, May 2023. [Online]. Available: http://arxiv.org/abs/2305.05974

[47] D. Chicco, V. Starovoitov, and G. Jurman, "The Benefits of the Matthews Correlation Coefficient (MCC) over the Diagnostic Odds Ratio (DOR) in Binary Classification Assessment," *IEEE Access*, vol. 9, pp. 47112–47124, 2021, doi: 10.1109/ACCESS.2021.3068614.